Feasibility study on the seismic isolation of pool-type LMFBR
2. Development of a rubber bearing and a friction damper

M.Kurihara & H.Kasai
Mechanical Engineering Research Laboratory, Hitachi Ltd, Tsuchiura, Japan
M.Madokoro & T.Yashiro
Hitachi Works, Hitachi Ltd, Japan
A.Yasaka & K.Odaka
Kajima Corporation, Tokyo, Japan

1. INTRODUCTION

Development of seismic isolation devices is a most important factor for the realization of a seismic isolation system in FBR plants. In this study, the seismic isolation system is composed of laminated rubber bearings and energy absorbers. A friction damper is adopted as an energy absorber. The friction damper is able to be designed to provide large energy absorption capability. However, the radical change in friction force excites the high frequency vibration modes of the building (Kurihara 1986). A modified friction damper with an initial soft stiffness to reduce the radical change in the damping force has thus been designed. To investigate the feasibility of applying rubber bearings and modified friction dampers to a seismic isolation system in FBR plants, loading and shaking table tests were performed using scale models. This paper describes: 1) the fracture characteristics of rubber bearings after aging tests and fatigue tests; 2) the dynamic characteristics and durability of the modified friction damper; and 3) the vibration characteristics of the seismic isolation system.

2. LOADING TESTS OF THE RUBBER BEARING

2.1 Scale model and experimental method

Specifications of the laminated rubber bearing for an actual plant are shown in Table 1. To estimate its fracture characteristics, aging and fatigue tests, and fracture loading tests were carried out using 1/11 scale models. These scale models are shown in Fig. 1 and the testing apparatus is shown in Fig. 2. The rubber bearings were put in a room with a constant temperature of 90°C under the static compression load of 4.1 ft to simulate the plant lifetime.

2.2 Test results

The restoring force characteristics of the rubber bearing, to the allowable displacement, is shown in Fig. 3. The observed result is somewhat small in comparison to the designed value. For example, at the rated displacement of 10 mm, which corresponds to the maximum response displacement arising from an artificial earthquake motion (Sonoda 1986), the spring constant of the rubber bearing is smaller by 14%. However, the difference is negligible in a practical application. Load displacement characteristics for each experimental condi-

tion during the fracture are shown in Fig. 4. The spring constants of the rubber bearings in the allowable displacement after aging tests rise slightly, compared with that for rubber bearings experiencing no aging. The fracture displacement of a rubber bearing after aging tests comparable to 60 years plant life is smaller by 30% than that with no aging. However, this value is greater than the allowable displacement by 30%. Therefore, it is found that the increase in spring constant and the decrease in fracture displacement of the rubber bearing over a plant's lifetime does not appear to be serious in a practical application.

Table 1 Design specificatoins for a rubber bearing

Loading Weight W (tf)		500
Natural Freq. (Hz)	Horizontal f_2	0.5
	Vertical fv	20
Spring Const. (tf/cm)	Horizontal K_2	4.85
	Vertical Kv	8180
Allowed Value of Horizontal Deformation Δa (cm)		50

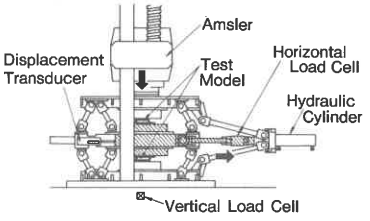

Fig. 2 Testing apparatus for rubber bearings

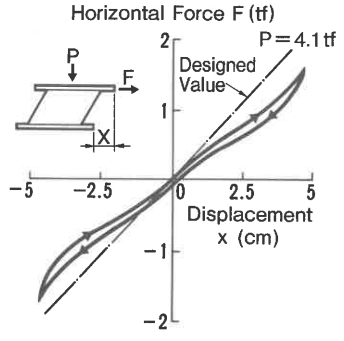

Fig. 3 Force-displacement relation of a rubber bearing

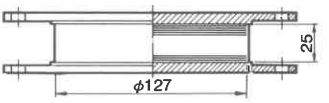

Horizontal Spring Const. : $K_2 = 439$ kgf/cm
Vertical Sping Const. : $Kv = 7.39 \times 10^5$ kgf/cm
Allowed Value of
Horizontai Displacement : $\Delta a = 4.6$ cm
Rubber: 1mm×17, Steel : 0.5mm×16

Fig. 1 Scale model of a rubber bearing

	Aging Condition of Model	Fatigue test Condition		
		Amplitude (mm)	Frequency (Hz)	Cycle
Ⓐ	No-Aging	10	0.5	10^4
Ⓑ	No-Aging	1	5	10^7
Ⓒ	40 Years Aging	1	5	10^7
Ⓓ	60 Years Aging	1	5	10^7
※	No-Aging	No-Fatigue		

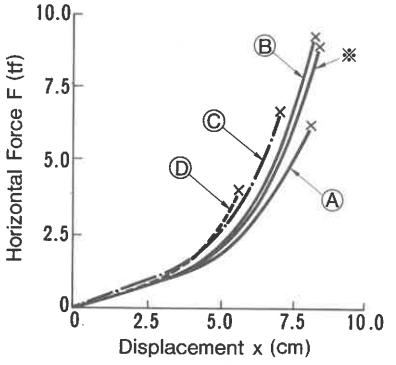

Fig. 4 Fracture characteristics of rubber bearings

3. LOADING TESTS OF THE MODIFIED FRICTION DAMPER

3.1 Scale model and experimental method

A diagram of the modified friction damper is shown in Fig. 5. This damper, which has elasto-plastic hysteresis characteristics, is characterized by the thin rubber layer called a pot bearing in series with friction plates. The plates

composed of a stainless steel plate and a brake pad are given a constant compressive load by the coned disc springs.

Loading tests for the damper were carried out with the testing apparatus shown in Fig. 6. The load-displacement characteristics and durability of the damper were investigated. In addition, conditions employed in the tests were a frequency of 0.5 Hz and a surface pressure of 100 kgf/cm^2.

3.2 Experimental results

The displacement effect on the spring constant of the pot bearing is shown in Fig. 7. The restoring force characteristics of the pot bearing at frequency 0.5 Hz are also given. The difference between the designed spring constant and the experimental result at a rated displacement of 0.91 mm is 10% at most. Therefore, the experimental result is considered to agree well with the designed value. The hysteresis loop of the damper at frequency 0.5 Hz is shown in Fig. 8. The displacement effect on the damping characteristics is shown in Fig. 9. From this figure, it can be seen that the friction force is almost constant, and that the loss energy increases in proportion to displacement. Therefore, it is found that the damper has stable damping characteristics at least to the same degree as the allowable displacement for the rubber bearing. The damper's durability for cyclic loading is shown in Fig. 10. The friction force increases slowly as the number of cycles increases, which means that the loss energy tends to increase as well. However, since the friction force increases by about 10% of the initial value at around one hundredth cycle, it is found that the damper is very durable as regards cyclic loading.

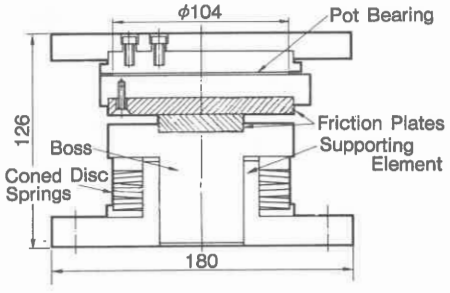

Fig. 5 Structure of the modified friction damper

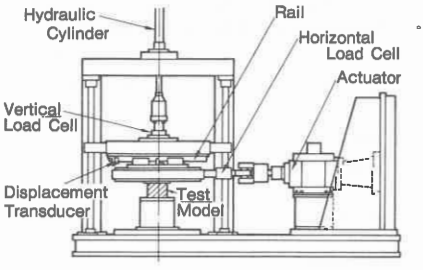

Fig. 6 Testing apparatus for dampers

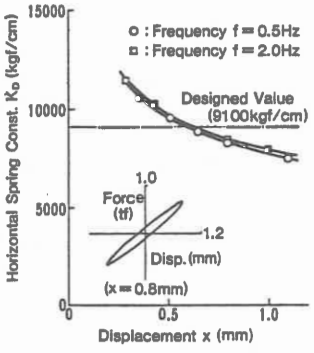

Fig. 7 Displacement characteristics of a pot bearing

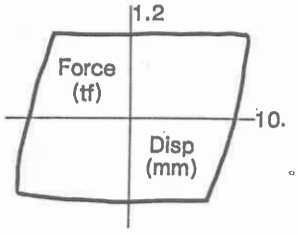

Fig. 8 Hysteresis loop of the modified friction damper

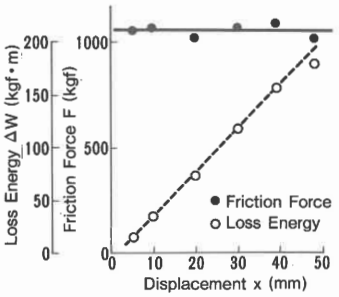

Fig. 9 Displacement characteristics of the modified friction damper

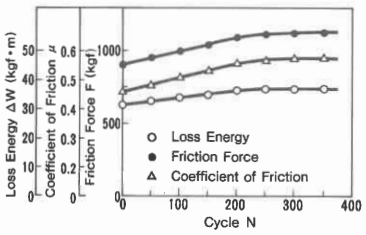

Fig. 10 Durability of the modified friction damper for cyclic loading

4. SHAKING TABLE TESTS

4.1 Isolated building model and experimental method

As shown in Fig. 11, the building model is a four-story, one-bay, steel-frame structure used to simulate vibration properties in the design model of a FBR building. The model is 18000 kgf in weight. The natural frequencies of the first and second modes of the model under a fixed base condition are 9.8Hz and 22.9Hz, respectively. The damping ratio of each mode is about 0.005. The model was mounted on four rubber bearings which had the same design specifications as those used in the loading tests. The first stiffness K_1, the second stiffness K_2 and the apparent yield force Q of the combined isolation device composed of four rubber bearings and two modified friction dampers were designed as shown in Table 2.

In order to obtain hysteresis characteristics of the combined isolation device, loading tests were performed using the hydraulic cylinder as shown in Fig. 11. Next, shaking table tests were carried out using the artificial earthquake motion that was reduced in time by $1/\sqrt{11}$ according to the similarity law.

4.2 Test results

The hysteresis loop of the combined isolation device is shown in Fig. 12. The isolation device operated as expected. Time histories of earthquake response accelerations on roof floor level and the relative displacement in the isolation story are shown in Fig. 13. Maximum response accelerations on each floor level are shown in Fig. 14. Also the results for an isolated building model with modified friction dampers is compared with those for one with ordinary friction dampers and a non-isolated building model. From Fig. 14, it can be seen that seismic isolation systems drastically reduce response accelerations when compared to a non-isolated type. However, the effectiveness in reducing response accelerations depends on the type of damper employed. In Fig. 14, one can see that the modified friction damper reduces response acclerations on each floor level by 1/2, compared with the ordinary friction damper. The relationship between the response acceleration on the second floor, the installation level of the reactor, and maximum input acceleration level is shown in Fig. 15. Floor response spectra on the second floor are shown in Fig. 16. The relationship between the floor response spectra on the second floor above the 5 Hz frequency and maixmum input acceleration level is shown in Fig. 17. From Fig. 16 and 17, it can be seen that the floor response spectra for the modified friction damper are less than 1/2 of those for the ordinary

friction damper, except in the neighborhood of the first mode. Therefore, supplying suitable elasto-plastic hysteresis characteristics to an ordinary friction damper is effective in reducing floor response spectra.

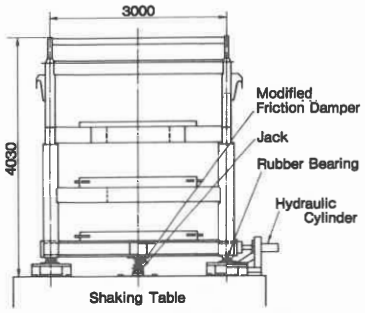

Fig. 11 Isolated building model

Table 2 Design specifications for the isolation device

	Designed Specification	
	Scale Model	Actual Model
K_1 (kgf/cm)	7,260	79,900
$\omega_1=\sqrt{K_1 g/w}$	3.3	1.0
K_2 (kgf/cm)	1,760	19,400
$\omega_2=\sqrt{K_2 g/w}$	1.6	0.5
Q (kgf)	825	100,000
$\beta=Q/w$	0.05	0.05

K_1 : First Stiffness Q : Apparent Yield Force
K_2 : Second Stiffness w : Weight of Building Model

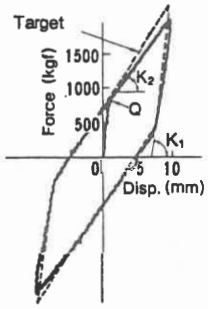

Fig. 12 Hysteresis loop of the isolation device

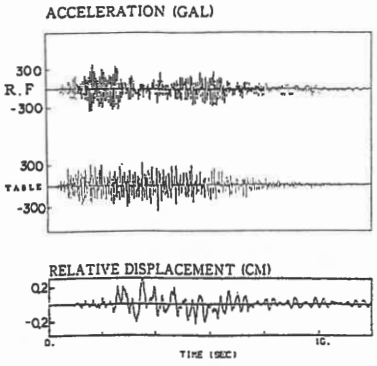

Fig. 13 Response waves of the isolated model with the modified friction damper

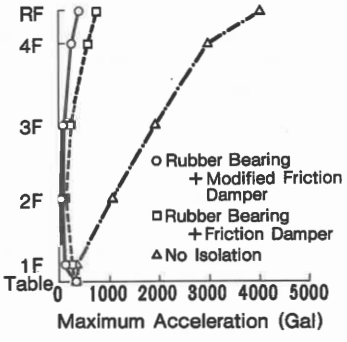

Fig. 14 Maximum response acceleration distribution

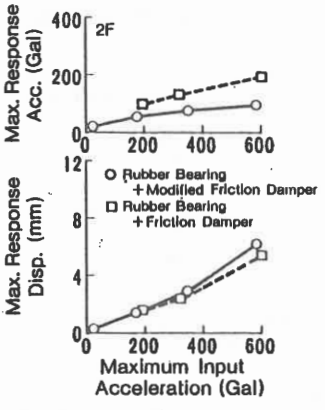

Fig. 15 Relationship between maximum response and maximum input acceleration

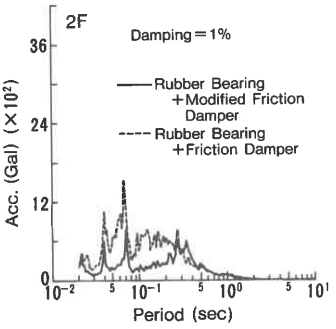

Fig. 16 Response spectra on 2nd floor (maximum input acc.=351 Gal)

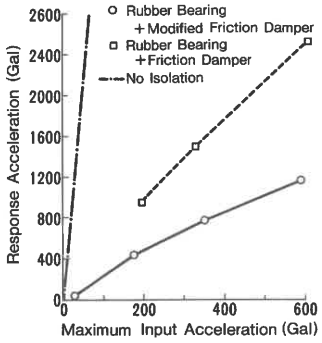

Fig. 17 Relationship between maximum response spectra on 2nd floor above 5Hz and maximum input acceleration

In this paper, simulation analysis results are abbreviated, but they agree approximately well with test results.

5. CONCLUSIONS

This paper presents a study on the feasibility of a seismic isolation system composed of rubber bearings and modified friction dampers for FBR buildings. The following conclusions are reached on the basis of loading and shaking table tests of the isolation device.

1. The increase in spring constant and the decrease in fracture displacement of a rubber bearing aged 60 years does not appear to be serious in a practical application.

2. The modified friction damper has almost ideal elasto-plastic hysteresis characteristics in a large displacement range and shows good durability for cyclic loading.

3. It is recognized that the modified friction damper greatly controls the excitation of high frequency vibration modes in isolated buildings.

4. The bilinear hysteretic parameters of the isolation device can be designed independently and accurately. Consequently, it is expected that a seismic isolation system which has the adequate hysteresis characteristics can applied to FBR buildings.

REFERENCES

Kurihara, M., et al., 1986. Feasibility study of a seismic isolation system for fast breeder reactor plants 2. Proc. of the 7th Japan earthquake engineering symposium: 1657 - 1662.

Sonoda, Y., et al., 1986. Feasibility study of a seismic isolation system for fast breeder reactor plants 1. Proc. of the 7th Japan earthquake engineering symposium : 1651 - 1656